

Absorption of Sulphur Dioxide with Sodium Hydroxide Solution in Packed Columns

By M. Schultes *

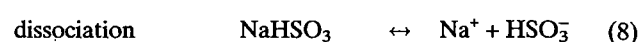
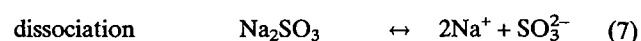
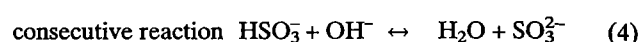
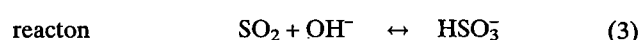
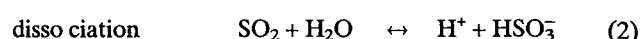
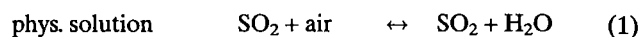
1 Introduction

The absorption of sulphur dioxide from effluent gases by using aqueous sodium hydroxide solution as a solvent has become established practice in industry where a high degree of purity of the effluent gases must be ensured in a reliable manner. Although it has long been known that it is basically possible to clean effluent gases containing sulphur dioxide effectively by using sodium hydroxide solution, there are only few publications to date which discuss the reaction-kinetic processes in the wash solution.^[5,9,11,14,17] An analysis of these publications clearly reveals that a number of experimental studies have been conducted under framework conditions far removed from those found in the practice of effluent gas purification. Thus, *Onda* et al. and *Vazquez* et al. conducted absorption tests with a gas phase of pure SO₂, although SO₂ concentrations in industrial effluent gas purification are lower. *Hikita* et al. obtained from theoretical derivations with predetermined boundary conditions mathematical solutions for the reaction-kinetic processes in the alkaline solution which are only met in limiting cases. In the publications to date it was always assumed that the reactions in the washing agent took place very rapidly, but this too holds only under certain conditions.

2 Reaction Sequences in Countercurrent Absorption

When SO₂ is absorbed in sodium hydroxide solution the SO₂ molecules first diffuse from the core current of the gas to the gas-liquid interface and dissolve in the washing agent according to the equality of the chemical potentials in the phases. In view of the low SO₂ concentrations predominant in effluent gases in practice, this means that Henry's law describes the relationship between the liquid concentration and the equilibrium partial pressure in the gas phase. It is only after this phase transition of the SO₂ molecules has taken place according to Eq. (1) that one observes a diffusion current toward the core of the phase, a dissociation according to Eq. (2), and the reaction with OH⁻ ions according to Eq. (3), whereby hydrogen sulfite reacts in turn with additional OH⁻ ions to sulfite as shown in Eq. (4). The reaction-

kinetic processes are also influenced by the dissociation of the water according to Eq. (5), of the sodium hydroxide solution according to Eq. (6) and of the sodium sulfite/hydrogen sulfite portions according to Eqs. (7) and (8), which are formed products.



In the case of countercurrent absorption in dumped-packing columns the fresh sodium hydroxide solution is introduced at the top of the column while the charged effluent gas is fed in at the bottom and discharges on the way to the top of the column. The result of this is that at the top of the absorber the fresh sodium hydroxide solution comes into contact with only mildly concentrated effluent gas, whereas in the bottom, largely spent solvent is faced with a charged gas stream. The result of this circumstance is that in certain column segments certain partial reactions of Eqs. (2)–(8) mainly occur and determine the mass transfer rate. This is to be explained with the help of Fig. 1. The fresh sodium hydroxide solution is strongly alkaline owing to the dissociation into Na⁺ and OH⁻ ions, and at the top of the column it presents a surplus to the quantity of SO₂ absorbed there. The SO₂ molecules dissolved in the liquid thus react according to Eqs. (3) and (4) according to the sum reaction of Eq. (9).



As the stream passes through the column, OH⁻ ions are continuously used up according to Eq. (9) so that the pH of the solution decreases. The conversion of the OH⁻ ions to SO₃²⁻, or of the sodium hydroxide solution to sodium sulfite, is complete at a pH of approx. 8.5. In the following, the sulfites dissociate according to Eq. (4) back to form hydrogen sulfite and OH⁻ ions whereby the latter continue to react with SO₂ according to Eq. (3) to form hydrogen sulfite. In

[*] Privatdozent Dr.-Ing. M. Schultes, Raschig AG, Mundenheimerstr. 100, 67061 Ludwigshafen GVC-Jahrestagung, 29./30. April 1996, Luzern/Schweiz.

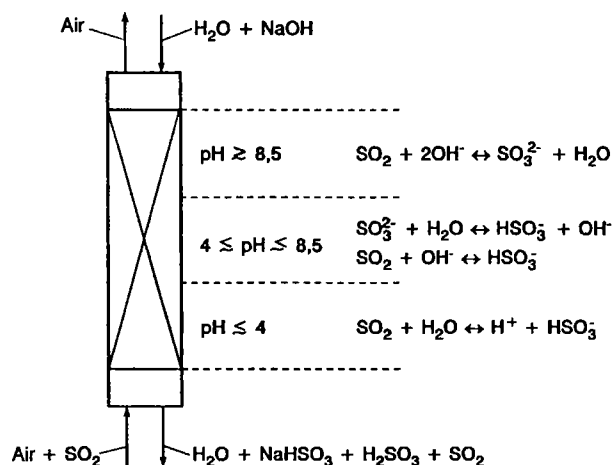


Fig. 1. Classification of the reactions decisive for the absorption of SO₂ in sodium hydroxide solution in various height segments of the mass transfer column.

this segment of the column, the pH decreases from 8.5 to 4. The separation of SO₃²⁻ in this pH range is determined by the reaction according to Eq. (3). In the acid range starting at pH ≈ 4 the dissociation of the sulphites is complete and the OH⁻ concentration negligible. For this reason, in the segment of the column with pH lower than 4, only the dissociation of the SO₂ molecules in water to H⁺ and HSO₃⁻ according to Eq. (2) occurs. Then the acid wash solution, with portions of sodium hydrogen sulfite, sulphurous acid, and physically solute sulphur dioxide, flows from the bottom of the column.

3 Reaction-kinetic Principles

The above illustrates that the mass transfer from SO₂ into sodium hydroxide solution is determined both by diffusion and by reaction processes. In order to describe the mass transfer rate it is, therefore, assumed that the total stream of \dot{n}_{SO_2} absorbed from the gas phase into the washing liquid is brought about by a diffusion current of physically solute SO₂ molecules $\dot{n}_{\text{SO}_2, \text{Diff}}$ and a mass transfer rate caused by chemical reactions $\dot{n}_{\text{SO}_2, \text{React.}}$, see Eq. (10).^{[6]1)}

$$\dot{n}_{\text{SO}_2} = \dot{n}_{\text{SO}_2, \text{Diff}} + \dot{n}_{\text{SO}_2, \text{Re ac.}} \quad (10)$$

$$\dot{n}_{\text{SO}_2} = \left(1 + \frac{\dot{n}_{\text{SO}_2, \text{Reac.}}}{\dot{n}_{\text{SO}_2, \text{Diff}}} \right) \dot{n}_{\text{SO}_2, \text{Diff}} = E \dot{n}_{\text{SO}_2, \text{Diff}} \quad (11)$$

$$\dot{n}_{\text{SO}_2} = E (\beta_L a_{\text{Ph}}) (c_{\text{SO}_2, \text{Ph}} - c_{\text{SO}_2, \delta}) \quad (12)$$

Eq. (10) can also be converted into the form of Eq. (11) in which the bracketed expression is defined as the enhancement factor E and describes the increase in the mass transfer

rate resulting from the reaction in comparison with the pure diffusion current. The mass transfer rate with the chemical reaction can then be expressed with the help of Eq. (12) in which $[c_{\text{SO}_2, \text{Ph}} - c_{\text{SO}_2, \delta}]$ describes the concentration gradient of the SO₂ molecules of the liquid phase-boundary layer and $\beta_L a_{\text{Ph}}$ describes the volumetric mass transfer coefficient in the liquid phase. The enhancement factor E depends decisively on the reaction equilibrium and on the reaction velocity, whereby the further the reaction equilibrium lies on the side of the reaction products and the faster the reactions rate, the larger is the enhancement factor.

A characteristic number for the assignment of reaction velocities is the Hatta number, which in its general form is defined according to Eq. (13) and places the maximal mass transfer rate by reaction in ratio to that resulting from diffusion. In Eq. (13) k_2 describes the velocity constant of a second-order reaction, $c_{\text{B}, \delta}$ the concentration of the reactant in the core of the phase, D_{SO_2} the diffusion coefficient, and β_L the mass transfer coefficient for sulphur dioxide in the solution. Tab. 1 shows the corresponding values of the Hatta numbers for the velocities of a reaction.

$$\text{Ha} = \frac{\sqrt{k_2 c_{\text{B}, \delta} D_{\text{SO}_2}}}{\beta_L} \quad (13)$$

Table 1. Classification of the reaction velocities in ranges of different Hatta numbers.

Ha < 0.02	very slow reaction
0.02 < Ha < 0.3	slow reaction
0.3 < Ha < 3	moderateley fast reaction
3 < Ha	fast reaction
E _i ≪ Ha	instantaneous reaction

4 Description of the Mass Transfer Rate in SO₂ Absorption with Sodium Hydroxide Solution

In the case of flue-gas desulfurization with sodium hydroxide solution the reactions of Eqs. (2) and (3) with the secondary reaction of Eq. (4) determine the mass transfer rate with sulphur dioxide. Since the secondary reaction of the ions according to Eq. (4) takes place much faster than the rate of Eq. (3), Eq. (3) determines the velocity of the reaction of the SO₂ molecules with the OH⁻ ions.^[5, 17] Whereas the reaction according to Eq. (2) is a pseudo first-order reaction with the velocity constant k_1 due to the large water surplus in the liquid phase, the mass transfer rate of Eq. (3) takes place as a function of the concentration of OH⁻ ions in accordance with a second-order reaction with the constant k_2 . Both reactions take place in parallel to and independent from one another, so that the Hatta number for the SO₂ absorption with an effective reaction velocity k_{eff} can be formed according to Eq. (14) by adding the individual velocities.^[17]

1) List of symbols at the end of the paper.

$$Ha_2 = \frac{\sqrt{k_{\text{eff}} D_{\text{SO}_2}}}{\beta_L} \text{ with } k_{\text{eff}} = k_1 + k_2 c_{\text{OH}^-, \delta} \quad (14)$$

It has already been pointed out that, in addition to the reaction kinetics, the reaction equilibrium defines the enhancement factor. If the limiting case of an infinitely rapid reaction is assumed, this means the reaction equilibrium comes about in the instant the co-reactants meet. The enhancement factor is then independent of the velocity of the reaction and is determined exclusively by the reaction equilibrium. Under instantaneous reaction conditions the acceleration factor assumes its largest possible value $E = E_i$.

If we assume that the mass transfer rate in the liquid of a random packed column takes place transiently and the reactions take place instantaneously and reversibly, the differential Eq. (15) can be derived from a total mass balance of all sulphur containing components.^[12] Under stationary conditions Eq. (16) follows with the penetration hypothesis of Higbie for the acceleration factor E_i . E_i is accordingly defined by the ratio of the diffusion coefficients of the components and their concentration differences between the interface (index Ph) and the core of the phase (index δ). The latter are linked with one another via the reaction equilibrium.

$$D_{\text{SO}_2} \frac{\partial^2 c_{\text{SO}_2}}{\partial z^2} + D_{\text{HSO}_3^-} \frac{\partial^2 c_{\text{HSO}_3^-}}{\partial z^2} + D_{\text{SO}_3^{2-}} \frac{\partial^2 c_{\text{SO}_3^{2-}}}{\partial z^2} + D_{\text{NaHSO}_3} \frac{\partial^2 c_{\text{NaHSO}_3}}{\partial z^2} + D_{\text{Na}_2\text{SO}_3} \frac{\partial^2 c_{\text{Na}_2\text{SO}_3}}{\partial z^2} = \frac{\partial c_{\text{SO}_2}}{\partial t} + \frac{\partial c_{\text{HSO}_3^-}}{\partial t} + \frac{\partial c_{\text{SO}_3^{2-}}}{\partial t} + \frac{\partial c_{\text{NaHSO}_3}}{\partial t} + \frac{\partial c_{\text{Na}_2\text{SO}_3}}{\partial t} \quad (15)$$

$$E_i = 1 + \sqrt{\frac{D_{\text{HSO}_3^-} c_{\text{HSO}_3^-, \text{Ph}} - c_{\text{HSO}_3^-, \delta}}{D_{\text{SO}_2} c_{\text{SO}_2, \text{Ph}} - c_{\text{SO}_2, \delta}}} + \sqrt{\frac{D_{\text{SO}_3^{2-}} c_{\text{SO}_3^{2-}, \text{Ph}} - c_{\text{SO}_3^{2-}, \delta}}{D_{\text{SO}_2} c_{\text{SO}_2, \text{Ph}} - c_{\text{SO}_2, \delta}}} + \sqrt{\frac{D_{\text{NaHSO}_3} c_{\text{NaHSO}_3, \text{Ph}} - c_{\text{NaHSO}_3, \delta}}{D_{\text{SO}_2} c_{\text{SO}_2, \text{Ph}} - c_{\text{SO}_2, \delta}}} + \sqrt{\frac{D_{\text{Na}_2\text{SO}_3} c_{\text{Na}_2\text{SO}_3, \text{Ph}} - c_{\text{Na}_2\text{SO}_3, \delta}}{D_{\text{SO}_2} c_{\text{SO}_2, \text{Ph}} - c_{\text{SO}_2, \delta}}} \quad (16)$$

Thus, it is only in instantaneous reactions that the enhancement factor $E = E_i$ is solely dependent on the reaction equilibrium and diffusion coefficients, and is not a function of the Hatta number. The condition which must be met for this is $E_i \ll Ha$, cf. Table 1. If, on the other hand, the reaction velocities are lower, this criterion is no longer fulfilled, and the enhancement factor is lower. The transition zones be-

tween the various reaction types and including a very slow reaction are fluid and can only be calculated exactly by numerical solution of the differential equations. Baldi and Siccardi, however, derived the approximation relation from Eq. (17). It enables the range for $Ha \geq 1$ to be recorded with only very small deviations from the numerical solution.

$$E = 1 + (E_i - 1) \left(1 - \exp \left\{ \frac{1 - \sqrt{(1 + Ha^2)}}{E_i - 1} \right\} \right) \text{ for } Ha \geq 1 \quad (17)$$

If the enhancement factor E is known, the height of a random packed column necessary for a transfer task can be determined according to the HTU-NTU model, as Eq. (18) shows. The height H is calculated from the product of the number of mass transfer units in the gas phase NTU_{OV} and the height of a mass transfer unit in the gas phase HTU_{OV} . The latter is composed of the gas-phase and liquid-phase mass transfer unit HTU_v and HTU_L as well as the stripping factor λ . Here, λ describes the quotient of the SO_2 phase equilibrium He/p and the molar flow ratio \dot{L}/\dot{V} with He as the Henry constant p as the system pressure. The mass transfer units HTU_v and HTU_L are defined by the gas and liquid velocities u_v , u_L , the volumetric mass transfer coefficients $\beta_v a_{\text{Ph}}$, $\beta_L a_{\text{Ph}}$, and the enhancement factor E .

$$H = HTU_{\text{OV}} NTU_{\text{OV}} = (HTU_v + \lambda HTU_L) NTU_{\text{OV}} = \left(\frac{u_v}{\beta_v a_{\text{Ph}}} + \frac{He/p}{\dot{L}/\dot{V}} \frac{1}{E} \frac{u_L}{\beta_L a_{\text{Ph}}} \right) NTU_{\text{OV}} \quad (18)$$

More recent studies have shown that the volumetric mass transfer coefficients can best be calculated by Eqs. (19) to (23). They are dependent on the column loads u_L , u_v , the viscosities η_z , η_v , the densities ρ_L , ρ_v , the diffusion coefficients for SO_2 D_L , D_v , the column hold-up h_L , the hydraulic packing diameter d_h , the specific surface area of the packing a , and the void fraction ϵ as well as the interface a_{Ph} .^[2,3,4,15]

$$\beta_L a_{\text{Ph}} = C_L \left(\frac{g \rho_L}{\eta_L} \right)^{1/6} \left(\frac{D_L}{d_h} \right)^{1/2} a^{2/3} u_L^{1/3} \left(\frac{a_{\text{Ph}}}{a} \right) \quad (19)$$

$$\beta_v a_{\text{Ph}} = C_v \frac{1}{(\epsilon - h_L)^{1/2}} \frac{a^{3/2}}{d_h^{1/2}} D_v \left(\frac{u_v \rho_v}{a \eta_v} \right)^{3/4} \left(\frac{\eta_v}{D_v \rho_v} \right)^{1/3} \left(\frac{a_{\text{Ph}}}{a} \right) \quad (20)$$

$$h_L = \left(12 \frac{\eta_L u_L a^2}{g \rho_L} \right)^{1/3} \quad (21)$$

$$d_h = 4 \frac{\epsilon}{a} \quad (22)$$

$$\frac{a_{\text{ph}}}{a} = 1,5(\text{ad}_h)^{-0,5} \left(\frac{u_L d_h}{v_L} \right)^{-0,2} \left(\frac{u_L^2 \rho_L d_h}{\sigma_L} \right)^{0,75} \left(\frac{u_L^2}{g d_h} \right)^{-0,45} \quad (23)$$

5 Calculating the Diffusion Coefficients

The diffusion behavior of molecules or ions in a liquid or gaseous phase is described with the help of the diffusion coefficient which, together with the concentration gradient in the phase-boundary layer defines the strength of the diffusion current according to Fick's first law. The diffusion coefficient of molecules in air or water can be found in the relevant collections of tables and converted to other system conditions as tabulated with the help of the Nernst correlation or the Stokes-Einstein relation.^[10] Furthermore, semi-empirical relations, e. g., those of Fuller, Schettler, and Giddings or Wilke and Chang also enable a theoretical precalculation of the diffusion coefficient.^[18,19]

In the case of the diffusion behavior of ions it must be borne in mind that their flow is always influenced by the diffusion of other charge carriers. In the case of SO₂ absorption in the liquid phase, one must bear in mind therefore that, at every location in the liquid film, the sum of all positive and negative charges must be the same owing to the electroneutrality requirement, see Eq. (24), and the flow of ion diffusion may effect a different charge potential in the core of the phase than at the interface. Charge potential is to be understood here as the absolute value of the right hand or of the left hand side of Eq. (24). For the description of the mass transfer of the charge carriers Eq. (25) follows in analogy to Eq. (15) from the total mass balance of all ions.

$$c_{\text{H}^+} + c_{\text{Na}^+} = c_{\text{HSO}_3^-} + 2c_{\text{SO}_3^{2-}} + c_{\text{OH}^-} \quad (24)$$

$$\begin{aligned} D_{\text{H}} + \frac{\partial^2 c_{\text{H}^+}}{\partial z^2} - D_{\text{HSO}_3^-} \frac{\partial^2 c_{\text{HSO}_3^-}}{\partial z^2} - 2D_{\text{SO}_3^{2-}} \frac{\partial^2 c_{\text{SO}_3^{2-}}}{\partial z^2} \\ - D_{\text{OH}^-} \frac{\partial^2 c_{\text{OH}^-}}{\partial z^2} + D_{\text{Na}^+} \frac{\partial^2 c_{\text{Na}^+}}{\partial z^2} = \frac{\partial c_{\text{H}^+}}{\partial t} \\ - \frac{\partial c_{\text{HSO}_3^-}}{\partial t} - 2 \frac{\partial c_{\text{SO}_3^{2-}}}{\partial t} - \frac{\partial c_{\text{OH}^-}}{\partial t} + \frac{\partial c_{\text{Na}^+}}{\partial t} \end{aligned} \quad (25)$$

If we now assume a linear potential gradient in the phase-boundary layer, according to the film theory and under stationary conditions Eq. (26) follows, while taking into account Eqs. (24) and (25), for the flow \dot{N}_i of the individual ion. According to this, the ionic current is comprised of a diffusivity according to Fick's first law which is enhanced or reduced by the second additive term, which contains the potential gradient $d\phi/dz$ is carried out with the help of Eq. (28). Here F describes the Faraday constant, R the general gas constant, T the temperature, and z_i the valency of the ions.

If we apply the penetration hypothesis of Higbie, Eq. (29) follows from analogous observations for the effective diffusion coefficient with the potential gradient according to Eq. (30).

$$\dot{N}_i = D_i^0 \frac{dc_i}{dz} + z_i D_i^0 c_i \frac{F}{RT} \frac{d\Phi}{dz} = \underbrace{D_i^0 \left(1 + z_i c_i \frac{F}{RT} \frac{d\Phi}{dz} \frac{dz}{dc_i} \right)}_{D_{\text{eff},i}} \frac{dc_i}{dz} \quad (26)$$

$$D_{\text{eff},i} = D_i^0 \left(1 + z_i c_i \frac{F}{RT} \frac{d\Phi}{dz} \frac{dz}{dc_i} \right) \quad (27)$$

$$\frac{F}{RT} \frac{d\Phi}{dz} = \frac{\frac{d}{dz} \left(\sum_i z_i D_i^0 c_i \right)}{\sum_i z_i^2 D_i^0 c_i} \quad (28)$$

In case of infinite dilution, the diffusion coefficient of an ion D_i^0 can be determined according to a method of Vinograd and McBrain; see Eq. (31), in which λ^2 describes the conductivity of the ion.^[20] The effective diffusion coefficients calculated according to Eqs. (29) to (31) are, therefore, to be entered in Eq. (16) for the determination of the enhancement factor E .

$$D_{\text{eff},i} = D_i^0 \left(1 + z_i c_i \frac{F}{RT} \frac{d\Phi}{dz} \frac{dz}{dc_i} \right)^2 \quad (29)$$

$$\frac{F}{RT} \frac{d\Phi}{dz} = \frac{\frac{d}{dz} \left(\sum_i z_i \sqrt{D_i^0} c_i \right)}{\sum_i z_i^2 \sqrt{D_i^0} c_i} \quad (30)$$

$$D_i^0 = \frac{RT\lambda^2}{z_i F^2} \quad (31)$$

6 Calculating the Reaction and Phase Equilibrium

The concentrations of the ions in the core of the phase and at the interface are linked via the reaction equilibrium of Eqs. (32) to (37) with the SO₂ partions, and are heavily dependent on the pH of the solution. The same holds for the Na⁺ portion in the washing water which is calculated according to Eq. (38) from the total alkaline concentration introduced at the top of the column $c_B = \Sigma c_{\text{Na}}$ reduced by the nondissociated portion of sodium hydroxide solution c_{NaOH} .

sodium sulphite $c_{\text{Na}_2\text{SO}_3}$, and sodium hydrogen sulphite c_{NaHSO_3} . The dissociations of the sodium compounds are calculated from the equilibrium relations of Eqs. (35) to (37). Correlations for the determination of the equilibrium constants as a function of temperature are shown in Tab. 2.

$$K_1 = \frac{c_{\text{HSO}_3^-} c_{\text{H}^+} \gamma_{\text{HSO}_3^-} \gamma_{\text{H}^+}}{c_{\text{SO}_2} \gamma_{\text{SO}_2}} \quad [\text{mol/l}] \quad (32)$$

$$K_2 = \frac{c_{\text{SO}_3^{2-}} c_{\text{H}^+} \gamma_{\text{SO}_3^{2-}} \gamma_{\text{H}^+}}{c_{\text{HSO}_3^-} \gamma_{\text{SO}_3^-}} \quad [\text{mol/l}] \quad (33)$$

$$K_w = c_{\text{H}^+} c_{\text{OH}^-} \quad [\text{mol/l}]^2 \quad (34)$$

$$K_3 = \frac{c_{\text{OH}^-} c_{\text{Na}^+} \gamma_{\text{OH}^-} \gamma_{\text{Na}^+}}{c_{\text{NaOH}} \gamma_{\text{NaOH}}} \quad [\text{mol/l}] \quad (35)$$

$$K_4 = \frac{c_{\text{SO}_3^{2-}} c_{\text{Na}^+}^2 \gamma_{\text{SO}_3^{2-}} \gamma_{\text{Na}^+}^2}{c_{\text{Na}_2\text{SO}_3} \gamma_{\text{Na}_2\text{SO}_3}} \quad [\text{mol/l}]^2 \quad (36)$$

$$K_5 = \frac{c_{\text{HSO}_3^-} c_{\text{Na}^+} \gamma_{\text{HSO}_3^-} \gamma_{\text{Na}^+}}{c_{\text{NaHSO}_3} \gamma_{\text{NaHSO}_3}} \quad [\text{mol/l}] \quad (37)$$

$$c_{\text{Na}^+} = c_B - c_{\text{NaOH}} - 2c_{\text{Na}_2\text{SO}_3} - c_{\text{NaHSO}_3} \quad [\text{mol/l}] \quad (38)$$

Table 2. Temperature dependence of the equilibrium constants He^0 , K_w and K_1 – K_5 .^[5,13]

$\ln K_1 = (-10600/T_0 - 17800 T_1 - 272 T_2 + 0.85 T_0 T_3)/R$	
$\ln K_2 = (-40940/T_0 - 3650 T_1 - 262 T_2 + 1.35 T_0 T_3)/R$	
$\ln K_3 = 4009.3/(R T)$	
$\ln K_4 = -8233.3/(R T)$	
$\ln K_5 = 2723.3/(R T)$	
$\log K_w = 948.876 - 24746.26/T - 405.8639 \log(T) + 0.48796 T - 0.0002371 T^2$	
$\ln(\text{He}^0 \frac{M_L}{\rho_L}) = (-510/T_0 + 26970/T_1 - 155 T_2 + 0.0175 T_0 T_3)/R$	
$R = 8.31448 \text{ J/(mol K)}$	
$T_0 = 298.15 \text{ K}$	$T_1 = 1/T_0 - 1/T$
$T_2 = T_0/T - 1 + \ln(T/T_0)$	$T_3 = T/T_0 - T_0 T - 2 \ln(T/T_0)$

The activity coefficients γ take into account the deviations of the thermodynamic equilibrium of real mixtures from those of an ideally diluted solution and can be calculated for ions according to *Debye and Hückel* in accordance with Eq. (39) and for SO_2 according to *Harned and Owen* in accordance with Eq. (40) as a function of the ionic strength I of the solution.^[18, 19] The parameters A_0 , B_1 , and C_1 for the determination of the activity coefficients are compiled in Tab. 3.

$$\log \gamma_i = \frac{A_0 \sqrt{I}}{1 + B_1 \sqrt{I}} + C_1 I \quad (39)$$

$$\log \gamma_{\text{SO}_2} = 0.076 I \quad (40)$$

Table 3. Constants for calculating the activity coefficients.^[5,13]

	H^+	OH^-	HSO_3^-	SO_3^{2-}	Na^+
B_1	2.0	1.0	1.5	1.5	1.0
C_1	0.4	0.3	0.0	0.0	0.1

$A_0 = -49.17063 + 784.0113/T + 10.1068899 \ln(T) - 4.311501 (T/100) + 0.335985 (T/100)^2$
 $\gamma_{\text{NaOH}} = \gamma_{\text{Na}_2\text{SO}_3} = \gamma_{\text{NaHSO}_3} = 1$

The phase equilibrium for SO_2 over the sodium hydroxide solution is described by Henry's law according to Eq. (41) which states that the SO_2 concentration in the gas phase y_{SO_2} is directly proportional to the physically dissolved SO_2 portions c_{SO_2} . The sulfur dioxide molecules absorbed from the gas into the liquid is present not only in the form of physically dissolved SO_2 in the solution but also in ionized form as HSO_3^- and SO_3^{2-} , as well as in the sodium compounds as NaHSO_3 and Na_2SO_3 . The total quantity of sulphur bound in the solution is calculated, therefore, from Eq. (42). For the phase equilibrium Eq. (43) can be derived from Eq. (41), taking into account the reaction equilibrium and the electro-neutrality requirement.

$$y_{\text{SO}_2} = \text{He} \frac{M_L}{\rho_L} \frac{c_{\text{SO}_2}}{p_i} \quad (41)$$

$$c_S = c_{\text{SO}_2} + c_{\text{HSO}_3^-} + c_{\text{SO}_3^{2-}} + c_{\text{NaHSO}_3} + c_{\text{Na}_2\text{SO}_3} \quad (42)$$

$$y_{\text{SO}_2} = \frac{\text{He} M_L}{p_i \rho_L} \frac{c_{\text{H}^+}^2 \{ c_{\text{H}^+} + c_{\text{Na}^+} - c_{\text{OH}^-} \}}{K_1 c_{\text{H}^+} + 2K_1 K_2} \quad (43)$$

$$\log \frac{\text{He}}{\text{He}^0} = h I \quad (44)$$

The differing solubility of SO_2 in an electrolyte solution in comparison with its solubility in pure water can be taken into account by the desalting parameter h and the ionic strength I according to the empirical equation (44) of *Van Krevelen and Hofijzer*.^[6,16] In the SO_2 -air/sodium hydroxide solution system this leads to the Henry's law coefficient increasing as the ionic strength increases. The Henry's law constant with infinite dilution He^0 can be calculated as a function of the temperature following a correlation according to Tab. 2.

7 Discussion of the Experimental Investigations

The calculation model presented is to be verified with the help of the experimental investigations. As Fig. 1 shows, characteristic height segments, in which certain reactions decisively determine the mass transfer rate, are formed during the absorption of SO_2 in sodium hydroxide solution. The portions of these ranges in the total height of a column depends heavily on the sodium hydroxide solution concentration with which the SO_2 absorption is carried out.

If, for instance, the experimental system will operate with a large surplus of sodium hydroxide solution in comparison with the total molar quantity of SO_2 absorbed, the column is run exclusively with very high pH values and Eq. (9) describes the mass transfer rate. If, however, no sodium hydroxide solution is added to the washing water, it will be essentially the SO_2 dissociation according to Eq. (2) and the physical solubility of the SO_2 molecules according to Eq. (1) which determine the mass transfer rate. Any intermediate operating state can be achieved by adding a sodium hydroxide solution of different concentrations.

The experiments were, therefore, carried out with different sodium hydroxide solution concentrations between 0 mol/l and 0.9 mol/l. Larger mole fractions of sodium hydroxide solution were not examined since in the case of the 0.9 molar solution the very rapid mass transfer rate according to Eq. (9) was already so dominant that the resistance for the mass transfer rate along the experimental column lay exclusively in the gas phase. Furthermore, the influence of the temperature on the absorption was examined by conducting the experiments both at 20 °C and at 50 °C. On the basis of the experiments with the 0.9 molar sodium hydroxide solution and investigations with the CO_2 -air/water system first the mass transfer coefficients $\beta_{VA_{Ph}}$, $\beta_{LA_{Ph}}$ in the purely gas and liquid phases are determined. The enhancement factor E was then determined from all additional experiments. The results of an absorption test with a 0.01 molar sodium hydroxide solution at 20 °C are described by way of an example.

Fig. 2 explains the influence of the Hatta number Ha on the enhancement factor E . The acceleration factor in a reaction E_i of infinite velocity serves as the parameter. If there is a pseudo first order rapid reaction, i.e. $3 < Ha < E_i$, the points in the diagram coincide with the diagonals. The enhancement factor then receives the value $E = Ha$. If, however, $Ha \gg E_i$ we have an instantaneous reaction and the points coincide with the flat-ending curves. In this case $E = E_i$ holds for the acceleration factor.^[6]

Fig. 2 also contains the development of the enhancement factors along the experimental column with the absorption of SO_2 in a 0.01 molar sodium hydroxide solution. From the illustration we can see that in the uppermost height segment we have what is known as an "inhibited" reaction because we have there a surplus of sodium hydroxide solution in the solvent, owing to the low residual charge of the gas phase, and only part of the base can react with the SO_2 molecules

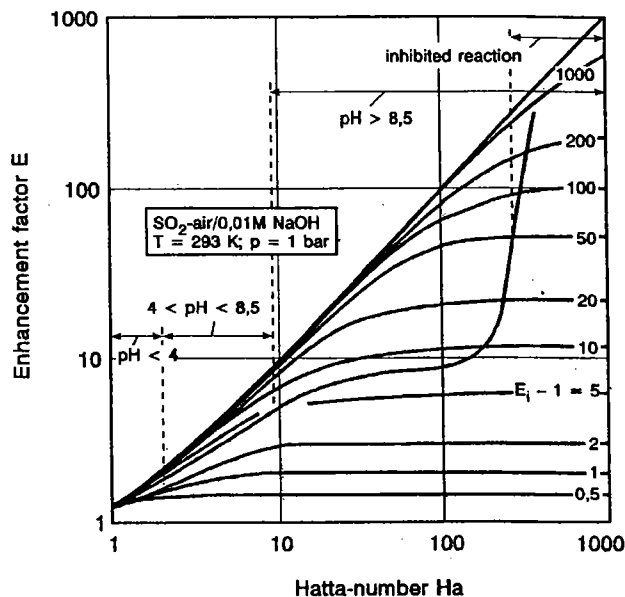


Fig. 2. Dependence of the enhancement factor E on the Hatta number Ha and on the enhancement factor in instantaneous reactions E_i .

diffusing into the liquid. The determinant reaction in this segment, Eq. (9), takes place so rapidly, however, and the enhancement factor assumes such large values, that the resistance for the mass transfer lies exclusively in the gas phase. The pH of the solution in this height segment lies around $\text{pH} = 12$.

On the liquid's path to the bottom of the column the SO_2 concentration in the gas rise and thus the stream of material diffusing into the solution increases. The reaction is, thus, accelerated and reaches for a brief time the range of the instantaneous reaction for which $E = E_i$ holds, i. e., the line intersects the flat branches of the curve. As more and more of the base is used up, the reaction slows down again and from now on always takes place in the transition zone between fast and instantaneous. In the case of very low pH values of below 4 it even drops into the only moderately rapid reaction range.

Fig. 3 shows the calculated concentration profiles along the column for the measurement point shown in Fig. 2. In the upper segment of the column, where Eq. (9) determines the mass transfer rate, the OH^- concentration drops dramatically and sulphite is formed in the core of the liquid phase. From a $\text{pH} \approx 8.5$ the SO_3^{2-} ions dissociate again according to Eq. (4) forming HSO_3^- and OH^- whereby the OH^- ions react with the SO_2 molecules to form hydrogen sulphite according to Eq. (3).

At the lower end of the mass transfer device from $\text{pH} \approx 4$ the HSO_3^- concentration continues to rise owing to the dissociation according to Eq. (2), and the SO_2 concentration in the liquid increases according to Eq. (1).

The meaning of these concentration profiles for the sizing of a mass transfer column is reflected in the height of a gas-phase mass transfer unit HTU_{OV} which is shown in Fig. 4 for the operating point observed along the column. The dia-

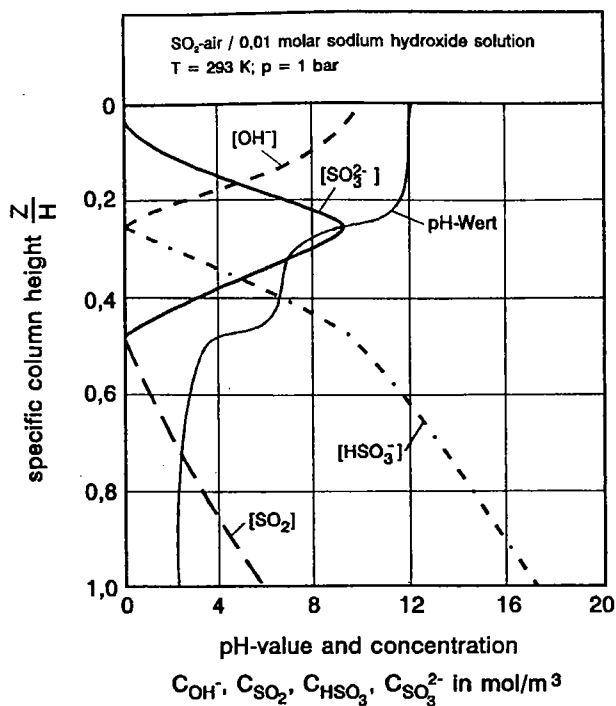


Fig. 3. Calculated concentration profiles along the height of a mass transfer column for a selected measurement point with 25 mm plastic Hiflow-Rings.

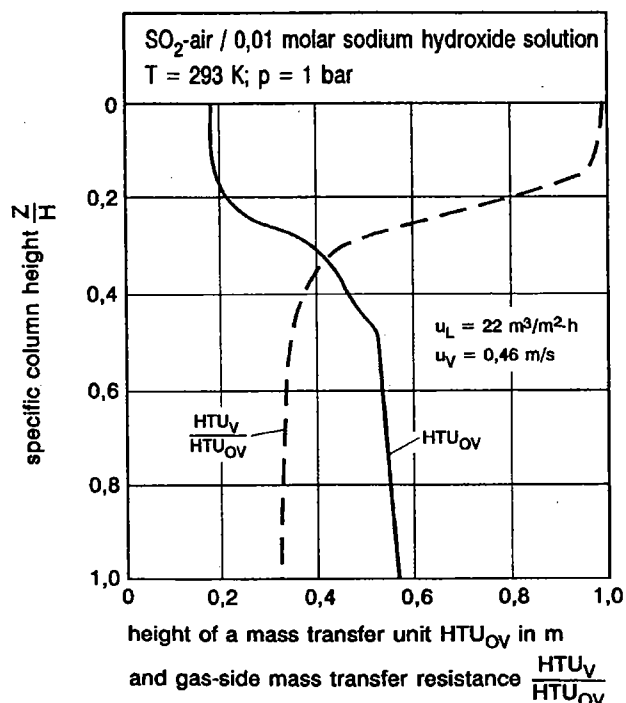


Fig. 4. Calculated gas phase mass transfer unit and gas phase resistance for the mass transfer along the height of a mass transfer column for a selected measurement point with 25 mm plastic Hiflow-Rings.

gram includes the resistance in the gas phase for the mass transfer HTU_V/HTU_{OV} . It can clearly be seen that in the upper segment of the column there is a resistance almost exclusively in the gas phase for the mass transfer, and the

HTU_{OV} values are very low. The resistance in the gas phase drops already in a height range in which very high pH values still predominate, i. e., the sulphite formation and the breakdown of the sodium hydroxide solution has not been completed. The HTU_{OV} values increase along the column to about triple and the mass transfer resistance in the gas phase drops to about 32%. The greatest changes take place in a pH range between 11.5 and 4, in which, for instance, the *Wellmann-Lord* process is used for desulfurization of flue gases. In this process, sodium sulphite is used for the absorption of SO_2 and is converted into sodium hydrogen sulphite.

The experimental investigations were conducted in an experimental column with a diameter of 0.16 m and a mass-transfer-efficient dumping height of 1.12 m and was filled with 25 mm Hiflow rings made of PVDF. The ambient air was first saturated with water vapor and charged with maximum 4% sulphur dioxide. Thereupon, the gas mixture flowed into the bottom of the column and upwards through the dumped packings.

The fresh sodium hydroxide solution prepared with deionized water was introduced at the top of the column via a liquid distributor with 2000 drainage points per m^2 cross-sectional area of the column and trickled down internally toward the gas stream.

The tests were conducted at 20 °C and 50 °C with various liquid and gas loads as well as six sodium hydroxide solution concentrations so that over 100 measurements were available for the verification of the model. The Hatta numbers were determined from the enhancement factors determined in the experiments with the help of Eq. (17) and the constants of the reaction velocities k_1 and k_2 according to Eq. (14). The evaluations showed that the constants k_1 and k_2 can be best described by Eqs. (45) and (46) as a function of the temperature T . On the basis of the measurements the k_2 values published by Wang and Himmelblau were confirmed.^[21] For the velocity constant k_1 in [l/s] Eigen^[17] gives the value 3.4×10^6 , Roberts and Friedländer^[14] 220, Phipps^[14] 2.8 and Wang and Himmelblau^[21] 2.2×10^{-2} at 20 °C, i. e., they differ by a total of 8 powers of ten. The value of Eq. (45) lies in the mid-range of the values given in the literature with $k_1 = 101$ l/s.

$$k_1 = 280 \exp\left(\frac{-300}{T}\right) \quad (45)$$

$$k_2 = 2738 \exp\left(\frac{3471}{T}\right) \quad (46)$$

On the basis of the calculation process described, the height of the dumped packings was precalculated theoretically according to Eq. (18) for the set experimental operating parameters, and compared with the mass-transfer-efficient dumping height installed in the experiment. The mean deviation between the calculated and the experimental heights was only 10%, whereby 80% of all the values com-

pared display a deviation of less than 15%. This good agreement confirms the algorithm of calculation presented.^[22]

In many desulfurization processes under industrial conditions, higher sodium sulphite concentrations are being used than described above. Under these process conditions it is shown that, even in the case of medium-range pH values, the influence of the mass transfer resistance in the gas phase on the SO₂ absorption rate prevails and the resistance in the liquid phase remains low. This relationship can also be taken into account in the calculation model if the velocity constant k_2 is also a function of the ionic strength. Analogous relationships were already recognized in the case of comparable chemical mass transfer rates. This still remains to be documented by additional investigations.

Finally, Figs. 5 and 6 illustrate once more the powerful influence of the enhancement factor and, in particular, of temperature on the gas phase mass transfer unit HTU_{OV} and on the gas phase mass transfer resistance HTU_V/HTU_{OV} . The diagrams were made for a plastic Ralu-Flow No. 2, whereby the volumetric mass transfer coefficients were calculated for an operating point at the loading point of the internals with the help of Eqs. (19) to (23).

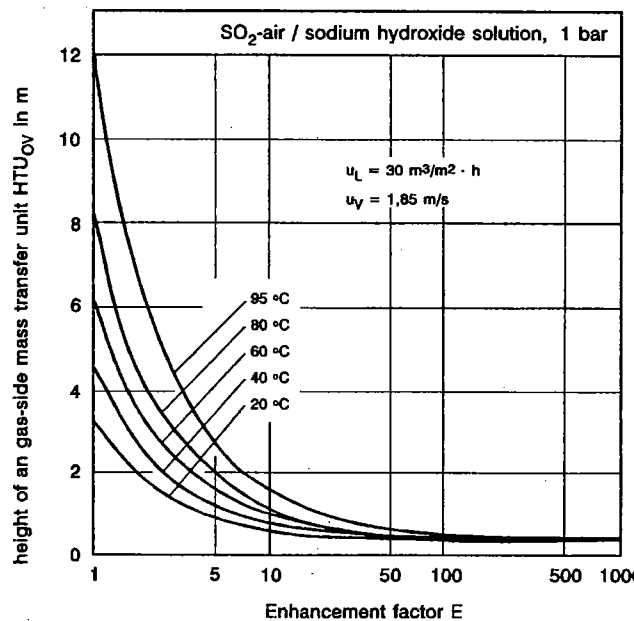


Fig. 5. Dependence of the height of a mass transfer unit on the temperature and on the enhancement factor in the case of chemical absorption of SO₂ in sodium hydroxide solution for a plastic Ralu-Flow No. 2.

It can clearly be seen that the E-factors below 100 lead to a very marked increase in the gas phase mass transfer units and to a serious drop in the gas phase mass transfer resistance. From both illustrations it can be seen that the changes increase as the absorption temperature increases. Fig. 5 illustrates furthermore that a constant HTU_{OV} value can be achieved at increasing absorption temperatures only with increasing enhancement factors, i. e., increased concentrations of sodium hydroxide solution.

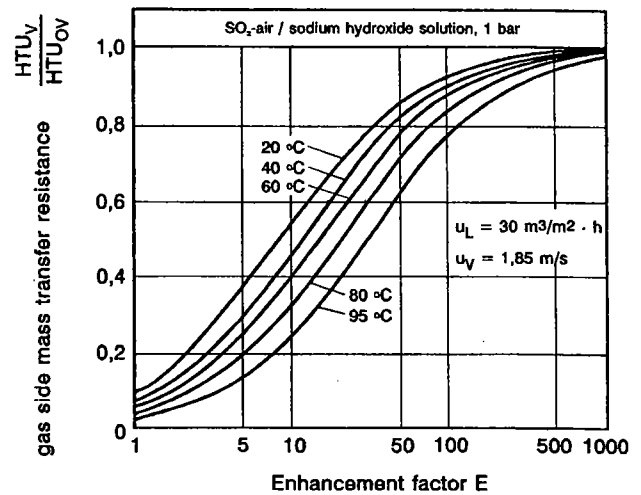


Fig. 6. Dependence of the distribution of resistance on the enhancement factor for the mass transfer of SO₂ in sodium hydroxide solution in the case of differing absorption temperatures for a plastic Ralu-Flow No. 2.

8 Conclusion

The theoretical calculation approaches presented and the experimental results described illustrate that, during the course of the purification of effluent gases containing sulphur dioxide with sodium hydroxide solution, the reaction velocities and reaction equilibrium in the solvent can change markedly. This must be taken into account in the sizing of flue gas desulfurization plants and leads to the conclusion that the height of a gas phase mass transfer unit increases and the gas phase mass transfer resistance along the path of flow of the liquid drops. The changes are dependent on the absorption conditions and increase as temperature rises. The experiments can be reproduced well with the help of the calculation methods described.

Received: May 5, 1997 [CET 912]

Symbols used

A_O	$[l/mol]^{0.5}$	Constant
a	$[m^2/m^3]$	Total surface area per unit packed volume
a_{Ph}	$[m^2/m^3]$	Effective interfacial area per unit packed volume
B_I	$[l/mol]^{0.5}$	Constant
c	$[kmol/m^3]$	Concentration in liquid
C_L, C_V		Constant
C_I	$[l/mol]$	Constant
d_H	$[m]$	Hydraulic diameter
D	$[m^2/s]$	Diffusion coefficient
E		Enhancement factor

F	[C/mol]	Faraday constant: F = 96485.31 C/mol
g	[m/s]	Gravitational constant
H	[m]	Height
Ha		Hatta number
He	[bar]	Henry constant
h_L	[m ³ /m ³]	Liquid hold-up
h	[l/mol]	Salting out parameter
I	[mol/l]	Molarity
HTU	[m]	Height of mass transfer unit
HTU _o	[m]	Overall height of mass transfer unit
K	[mol/l], [mol/l] ²	Equilibrium constant for reaction
k_1	[l/s]	Velocity constant for reaction
k_2	[m ³ /kmol s]	Velocity constant for reaction
\dot{L}	[kmol/h]	Molare flow of liquid
M	[kg/kmol]	Molecular weight
\dot{N}	[kmol/m ² s]	Molar flow of transferring component
\dot{n}	[kmol/m ³ s]	Molar flow of transferring component
NTU _o		Overall number of transfer unit
p	[bar]	Pressure
R	[J/mol K]	Natural gas constant
T	[K]	Temperature
t	[s]	Time
u_L	[m ³ /(m ² s)]	Liquid load
u_V	[m/s]	Superficial gas or vapor velocity
\dot{V}	[kmol/h]	Molare flow of gas or vapor
y	[kmol/kmol]	Mole fraction in gas or vapor phase
z	[m]	Coordinate
z_1		Valency of ion
β	[m/s]	Mass transfer coefficient
γ		Activity constant
ϵ	[m ³ /m ³]	Void fraction
η	[kg/m s]	Dynamic viscosity
λ		Stripping factor
λ^\pm		Conductivity of ion
ν	[m ² /s]	Kinematic viscosity
ρ	[kg/m ³]	Density
σ	[kg/s ²]	Surface tension
ϕ	[J/C]	Electrical potential

Subscripts

B	Base
eff	Effective
I	Ion
i	Instantaneous
L	Liquid
Ph	Interfacial area
V	Gas
W	Water
δ	Core of phase

References

- [1] Baldi, G.; Sicardi, S., *Chem. Eng. Sci.* 30 (1975) p. 617.
- [2] Billet, R., *Festschrift der Fakultät für Maschinenbau, Ruhr-Universität Bochum* (1983) p. 24.
- [3] Billet, R., *Fat. Sci. Technol.* 9 (1990) p. 361.
- [4] Billet, R.; Schultes, M., *Chem. Eng. Technol.* 16 (1993) p. 1.
- [5] Chang, C. S.; Rochelle, G. T., *Ind. Eng. Chem. Fundam.* 24 (1985) p. 7.
- [6] Dankwerts, P. V., *Gas-Liquid Reactions*, McGraw-Hill Chemical Engineering Series, 1970.
- [7] Doraiswamy, L. K.; Sharma, M. M., *Heterogeneous Reactions; Analysis, Examples and Reactor Design*, John Wiley & Sons New York, Vol. 2 (1984)
- [8] Harned, H. S.; Owen, B. B., *The Physical Chemistry of Electrolytic Solution*; 3rd Edition; Reinhold, New York 1958.
- [9] Hikita, H.; Asai, S.; Tsuji, T., *AIChE Journal* 23 (1977) No. 4, p. 538.
- [10] Hobler, T., *Mass Transfer and Absorption*, Pergamon Press, Frankfurt 1966.
- [11] Onda, K. T.; Kobayashi, T.; Fujine, M.; Takahashi, M., *Chem. Eng. Sci.* 26 (1971) p. 2009, p. 2027.
- [12] Olander, D. R., *AIChE J.* 6 (1960) p. 233.
- [13] Pasuik-Bronikowska, W.; Rudzinsky, K. J., *Chem. Eng. Sci.* 46 (1991) p. 2281.
- [14] Roberts, D. L.; Friedländer, S. K., *AIChE J.* 26 (1980) No. 4, p. 593.
- [15] Schultes, M., *Dissertation an der Ruhr-Universität Bochum 1990, Fortschritt-Berichte VDI-Reihe 3, Nr. 230, 4000 Düsseldorf 1, VDI-Verlag 1990.*
- [16] Van Krevelen, D. W.; Hofstijzer, P. J., *Int. Congr. Chim. Ind.*, 21st, Brussels Special No. (1948) p. 168.
- [17] Vaquez, G.; Antorrena, G.; Chenlo, F.; Paleo, F., *Chem. Eng. Technol.* 11 (1988) p. 156.
- [18] *VDI-Wärmeatlas* VDI-Verlag Düsseldorf (1991).
- [19] *Verfahrenstechnische Berechnungsmethoden; Teil 7, Stoffdaten*, VCH-Verlag Weinheim 1985.
- [20] Vinograd, J. R.; McBrien, J. W., *J. Am. Chem. Soc.* 63 (1941) p. 2008.
- [21] Wang, J. C.; Himmelblau, D. M., *AIChE J.* 10 (1964) p. 574.
- [22] Schultes, M., *Abgasreinigung*, Springer Verlag, Heidelberg 1996.